ChemPubSoc Europe

DOI: 10.1002/slct.201900558

Chemistry SELECT Full Papers

Materials Science inc. Nanomaterials & Polymers

An Ultra-sensitive, Rapidly Responsive Strain Sensor Based on Silver Microflakes by Simple Process

Shaocun Yan,[a, c] Muhammad Farooq Saleem,[a] Hongru Ma,[e] Zhe Li,[a, c] Xiao Zhang,[a] Xuhong Guo,[c, d] Yanqing Ma,*[a, b] and Lei Ma*[a]

Flexible sensors with excellent sensitivity and stable performance are attracting more and more attention in emerging electronics. Herein, silver microflakes (AgMFs) as conductive filler in polyaniline (PANI)/polyurethane (PU) matrix are used to prepare the AgMFs/PANI/PU strain sensor by simple mixing and curing process. The AgMFs/PANI/PU strain sensor has high sensitivity (GF = 173.66), ultra-short response time (10 ms), and reassuring cycle stability (> 4000 times). Excellent sensor performance demonstrates its unlimited potential for health monitoring, such as joint motion, breathing and pulse beat.

1. Introduction

In recent years, flexible strain sensors have developed rapidly. This kind of sensors are very important in many ways, such as wearable electronics,[1] artificial muscles,[2] human-machine interfaces,[3] and health monitoring (e.g., monitoring pulse, respiration, phonation, and movement).[4] These applications have great significance for the prevention and treatment of human diseases.[5]

Flexible polymer materials are often used in the preparation of flexible strain sensors. Wang[6] prepared a flexible pressure sensor based on a microstructure polydimethylsiloxane (PDMS) film. The pressure sensor has high stability and high sensitivity detection ability (-13 kpa^{-1}), wide working pressure range (0-4 kPa), and fast response (< 100 ms). Moon[7] added Ag flakes/Ag nanocrystals to the PDMS to prepare a strain sensor with a sensitivity factor of 7.1. The sensor has tensile mechanical stability of more than 10,000 times. Polyurethane have many advantages: high elasticity, easy processability, and good tensile strength.[8] On the other hand, the polyurethane can be flexibly designed suitable for application in different electronic devices.[9] Kang[10] reported a pressure sensor made from polyurethane sponge with a wide range of strains (0-75%), they also monitored human health. Liu[11] used PU to prepare piezoresistive sensors with good elasticity, fast response time (9 ms) and ultra-low detection limit (0.568 pa), and reproducibility over 1000 times. Grigoryev[12] has studied the optical and photoelectric properties of the zinc oxide film, indicating that the optical and photoelectric properties of the thin zinc oxide film are equivalent to that of the single crystal zinc oxide and can be used to make UV-photoresistors. Jagtap[13] prepared silver doped $CdS_{0.2}Se_{0.8}$ thin films, characterized for optoelectronic and physicochemical properties, confirms the size quantization of the particle while 1 wt% doping concentration of silver.

To meet the requirement of flexible strain sensor, a composite which has both good mechanical properties and good electrical conductivity, is usually fabricated by adding filler to a matrix.[14] Many conductive fillers are used to make highly sensitive sensors, such as flakes,[15] nanocrystals (NCs),[16] nanowires (NWs),[17] carbon nanotubes (CNTs),[18] or graphene.[19] Silver sheets are also used because of their good electrical conductivity and the ability to form a large number of pathways in polymer.[20] A kind of printable elastic conductor with silver flakes as conductive filler was reported, and a conductivity of 182 $S\,cm^{-1}$ at stretch to 215% strain was obtained.[21] Adding silver flakes to polyurethane, high tensile rate (600%) was obtained and in illuminating an LED at a strain (400%).[22] By adding silver nanoparticles into the silver flakes network, Kim[23] improved the cyclic stability of the strain sensor, and it could be stretched for more than 10000 times under 50% strain. Song[24] has prepared a polyurethane/silver nanowire high-performance strain sensor, which successfully combines high transparency, sensitivity, durability, self-healing and flexibility, showing good application potential. Bin[25] fabricated Ag nanodendrites strain sensors by directly screen-printing technology. By printing general geometry obtained different working strain ranges and sensitivity simultaneously.

Previous studies on flexible conductive materials have mostly focused on the modification of fillers, but the effect of matrix modification is still unknown.[20] The design of new

[a] S. Yan, M. F. Saleem, Z. Li, X. Zhang, Dr. Y. Ma, Prof. L. Ma
Tianjin International Center for Nanoparticles and Nanosystems,Tianjin University, Tianjin 300072, P. R. China
E-mail: mayanqing@tju.edu.cn
lei.ma@tju.edu.cn
[b] Dr. Y. Ma
State Laboratory of Precision Measuring Technology and Instruments, Tianjin University, Tianjin 300072, P. R. China
[c] S. Yan, Z. Li, Prof. X. Guo
School of Chemistry and Chemical Engineering, Shihezi University, Shihezi 832003, P. R. China
[d] Prof. X. Guo
State Key Laboratory of Chemical Engineering, East China University of Science and Technology, Shanghai 200237, P. R China
[e] H. Ma
State Key Laboratory of Fine Chemicals, School of Chemistry, Dalian University of Technology, Dalian, 116024, P. R. China

Supporting information for this article is available on the WWW under https://doi.org/10.1002/slct.201900558

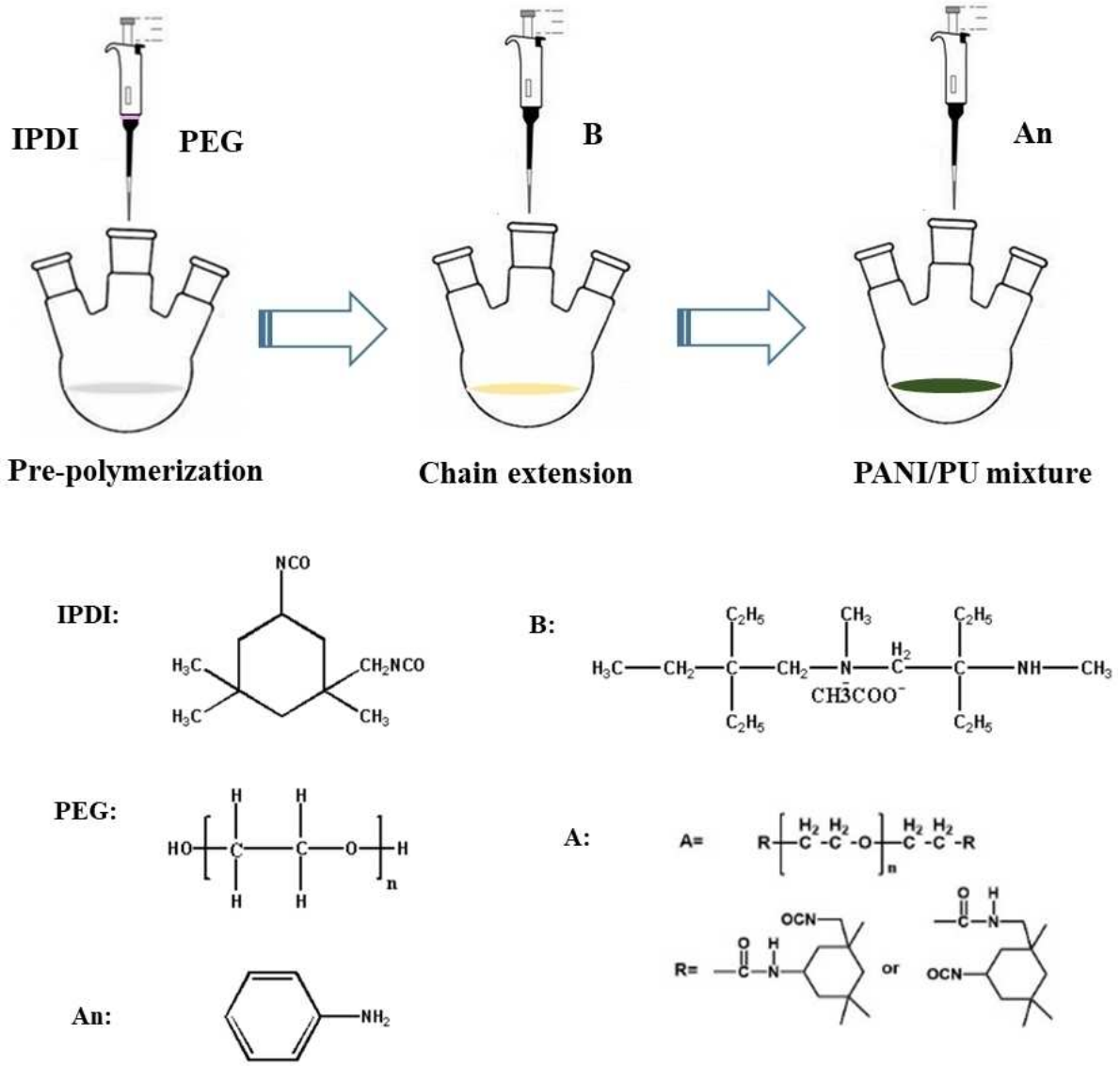

Figure 1. Schematic showing the synthetic step of PANI/PU mixture.

materials including optimization of the design of the conductive fillers and polymer matrix. The former can reduce the tunnel distance between the conductive filler and the latter can help to reduce the tunnel potential under deformation.[26] The addition of conductive polymers to the matrix provides additional carrier channels and significantly reduces contact resistance. Adding conjugated conductive polymer polyaniline (PANI) to polyurethane can increase the density of available states for charge transport and thus reduce the tunneling barrier.[27] PANI was added into PU matrix because of its relatively easy synthesis, low cost and good chemical and thermal stability.[28]

Until now, silver microflakes (AgMFs) mixed with PANI/PU polymeric base material flexible strain sensor is seldom reported. Silver flakes has good ductility and electrical conductivity,[29] while PANI/PU polymeric base material has excellent mechanical properties,[28] which are all suitable for high performance strain sensor. Herein, presented a simply yet effective method in the preparation of the AgMFs/PANI/PU flexible strain sensor (Figure 1 and Figure S1, Supporting Information). It has been used in human health monitoring, such as finger bend, blink, breath and pulse et al.

2. Results and Discussion

Our flexible sensor can be easily bent. Image shows the AgMFs uniformly dispersed in the PANI/PU matrix (Figure S2a, Supporting Information), which provides a major contribution to the formation of conductive pathways.[30] Under the bending condition (Figure S2b, Supporting Information), the channel remains its structure, which is the basis for the deformation sensor to have conductivity under deformation conditions. The proposed sensor is conducive to the stable long-term cycling of the sensor. The flexible AgMFs/PANI/PU film shows good

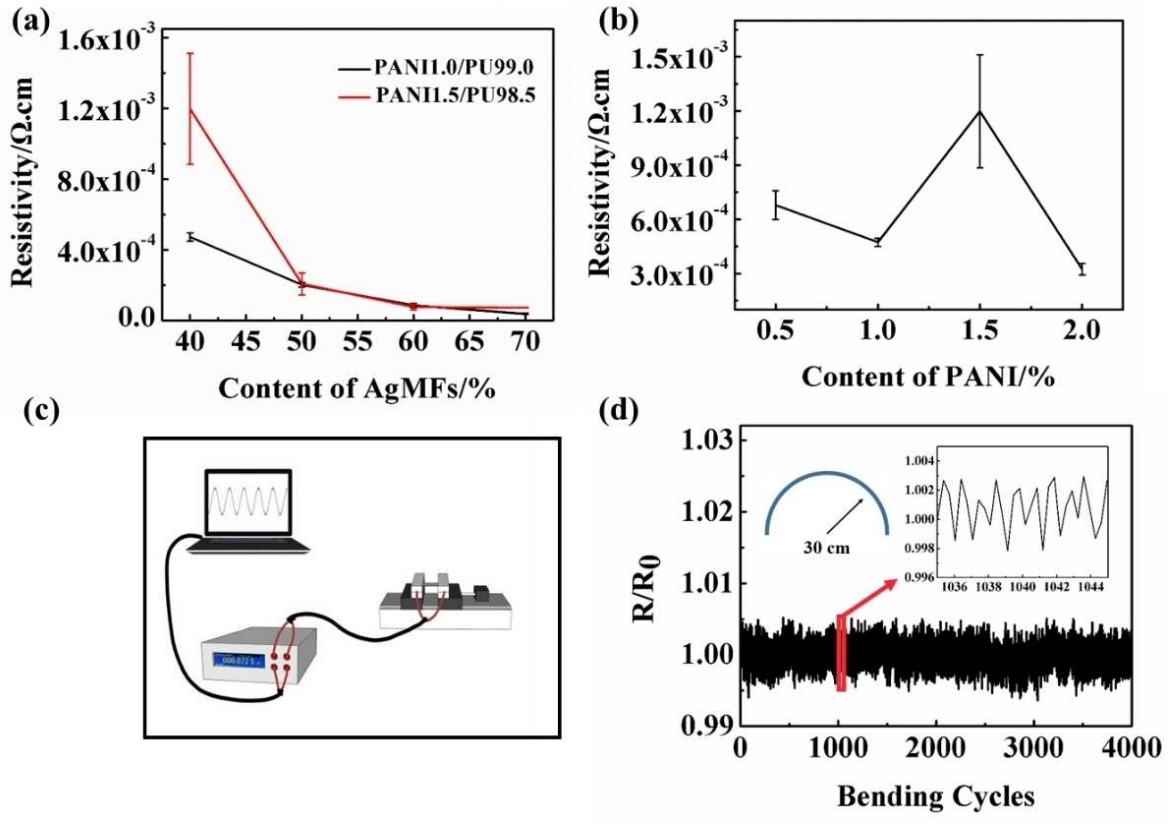

Figure 2. a) Resistivity of sensor-changing trend image under different content of AgMFs. (b) Resistivity of sensor-changing trend image under different content of PANI with 40% AgMFs sensor, (c) Test equipment drawing of the circulator; (d) the electrical resistance changes (R/R_0) of AgMFs/PANI/PU.

bendability and stable appearance (Figure S2c, S2d, Supporting Information). The goal we strive for is to be able to achieve the corresponding function under a variety of mechanical deformations.

The AgMFs/PANI/PU sample is composed of conductive filler (AgMFs) and matrix (PANI/PU). The conductivity is mainly provided by AgMFs. Meanwhile, the matrix also contributes to the conductivity due to the addition of polyaniline. The percolation theory holds that the contact between conductive fillers to form a conductive path is the reason for the conductive behavior of flexible conductive composites. The resistivity of flexible conductive composites is related to the content of conductive filler. When the content of conductive filler is low, the flexible conductive composite material is not conductive or has poor conductivity. When the content of the conductive filler reaches the percolation threshold, the conductive filler forms a continuous conductive path in the matrix. At this time, the resistivity of the flexible conductive composite material drops sharply and changes from an insulator to a conductor. The resistance value will decrease slightly and gradually become stable as the packing quantity continues to increase.[31] It can be seen from Figure. 2a that as the content of the conductive filler increases, the resistance value decreases. When the content of the conductive filler reaches 60%, there is an inflection point, and then the resistance decreases slowly or even no longer, we draw the conclusion that this inflection point is the threshold. Figure 2b shows the resistivity of different proportions of PANI in the matrix when the conductive filler is fixed at an additive level of 40%. When the content of polyaniline in the matrix is 1.5%, the sample shows relatively high resistivity. When the amount of conductive filler is high, many complete conductive paths are formed inside the sample, which suggests its application in the field of packaging.[32] However, the high sensitivity requires the condition that the small deformation of sample can produce high feedback. Therefore, to obtain better differential feedback, the sample should possess relatively weak conductive paths and show high resistivity.[14] The premise is to guarantee a certain path. For the above considerations, we select a sample with 40% conductive filler and a polyaniline content of 1.5% in the matrix. The cycle stability of the samples is measured on a self-made cycle stretcher. It shows stable performance of 4000 times with a bending radius of 30 cm, indicating that our sensor is very repeatable (Figure 2d). This proves that the strain sensors we have obtained are suitable for long-term deformation and have good development space in terms of cycle stability. The above tests were all implemented in the home-made loop resistance test system (Figure 2c).

We find that the AgMFs/PANI/PU strain sensors have the advantages of stable operation, high resolution and good repeatability. Figure 3 shows the variation of normalization resistance when the strain values of 2.26, 3.49, 4.37, 5.24, 6.12,

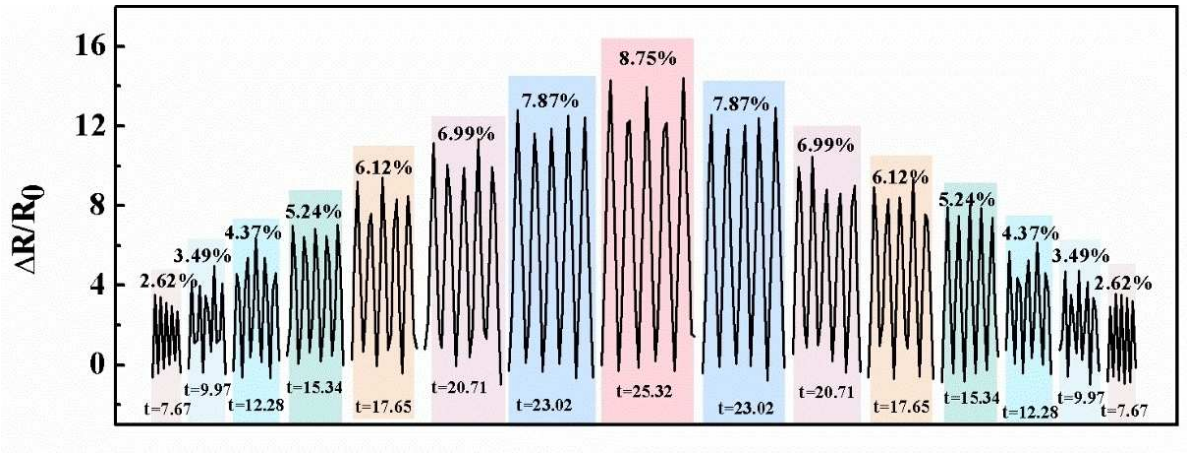

Figure 3. The normalization resistance of repeated strain of strain sensor under different strain

6.99, 7.87, and 8.75%. The detected limit of the flexible sensor is 0–8.75%. The normalization resistance increases as the strain value is increased and vice versa. The whole process is continuous, the variation law of gradient and symmetry show that the strain sensor has stable operation and resolution with good repeatability under different value of strain. Under a constant strain, the normalization resistance remains stable, which further proves that the sensor has good repeatability. The response to continuous stress reflects the sensor's dynamic response capability.[33]

The AgMFs/PANI/PU strain sensor is installed in a self-made tensile testing machine to record the change of electrical resistance under different strain. The gauge factor (GF) was obtained by recording and calculating, which is used to represent the sensitivity of the strain sensor. The GF[34] of the strain sensor is defined as:

$$GF = \frac{\Delta R/\ R_0}{\Delta L/\ L_0} = \frac{\Delta R/\ R_0}{\varepsilon} \quad (1)$$

Where ΔR and R_0 are the resistance variation and the initial resistance, $\Delta R/R_0$ is the normalized electrical resistance variation; ΔL and L_0 are the change in length and the original length; ε is the strain value.

The GF value is 173.66 shown in Figure 4. We summarize the results compared with other researchers (Table 1). Table 1 shows that the metal nanomaterials are generally highly sensitive and the sensitivity of the composite filler is particularly outstanding.[35] The tight connection between the fillers leads to small initial resistance.[36] This is the reason that the GF of AgMFs/PANI/PU strain sensor is as high as 173.66. The sensitivity and stability of the strain sensor is also related to the thickness of the film and the quantity factor of the filler.[34]

Flexible electronic devices can adapt to strains of various shapes, so they can be directly attached to the skin to accurately measure human motion and physiological activities.[43] The electrochemical workstation can well capture the change of weak current signal. Figure S3a in the Supporting

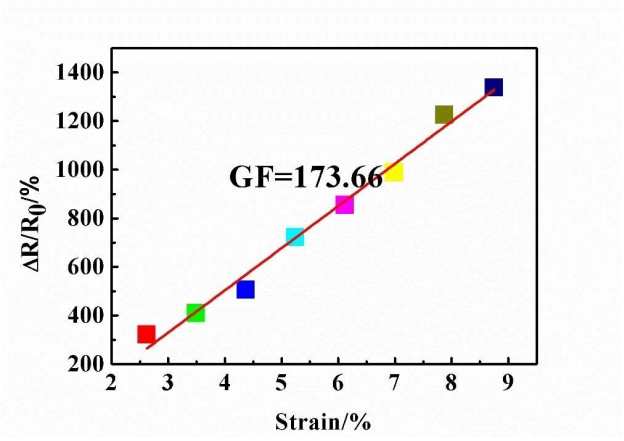

Figure 4. The relationship between of normalization and strain resistance

Table 1. Research status of reported flexible strain sensors

Materials	Gauge factor (strain)	Ref.
CNTs/Nonwoven	5.34 (1.8%)	[37]
CNTs& Graphene/PDMS	11.4 (9%)	[38]
Graphene/AgNPs/TPU	200 (2%)	[39]
CPC@PU yarn	70.6 (1%)	[40]
CNT yarn	0.5 (1%)	[1 f]
Graphene/AgNPs/TPU	333 (500%)	[35]
Ag NWs/PDMS	30 (%)	[41]
AgNWs + AgNPs/PDMS	3766 (28.1%)	[42]
Ag&CNTs/PDMS	20 (2%)	[16b]
AgMFs/PANI/PU	173.66 (8.75%)	This work

Information shows the working diagram of electrochemical workstation in health monitoring. Due to the irregular distribution of silver plates in the sensor, a microstructure network is automatically formed (Figure S3b, Supporting Information). When the sensor is attached to different parts of body, different deformation is caused by corresponding relative motion. The deformation leads to the change of the internal electrical network of the sensor, which results in the change of current

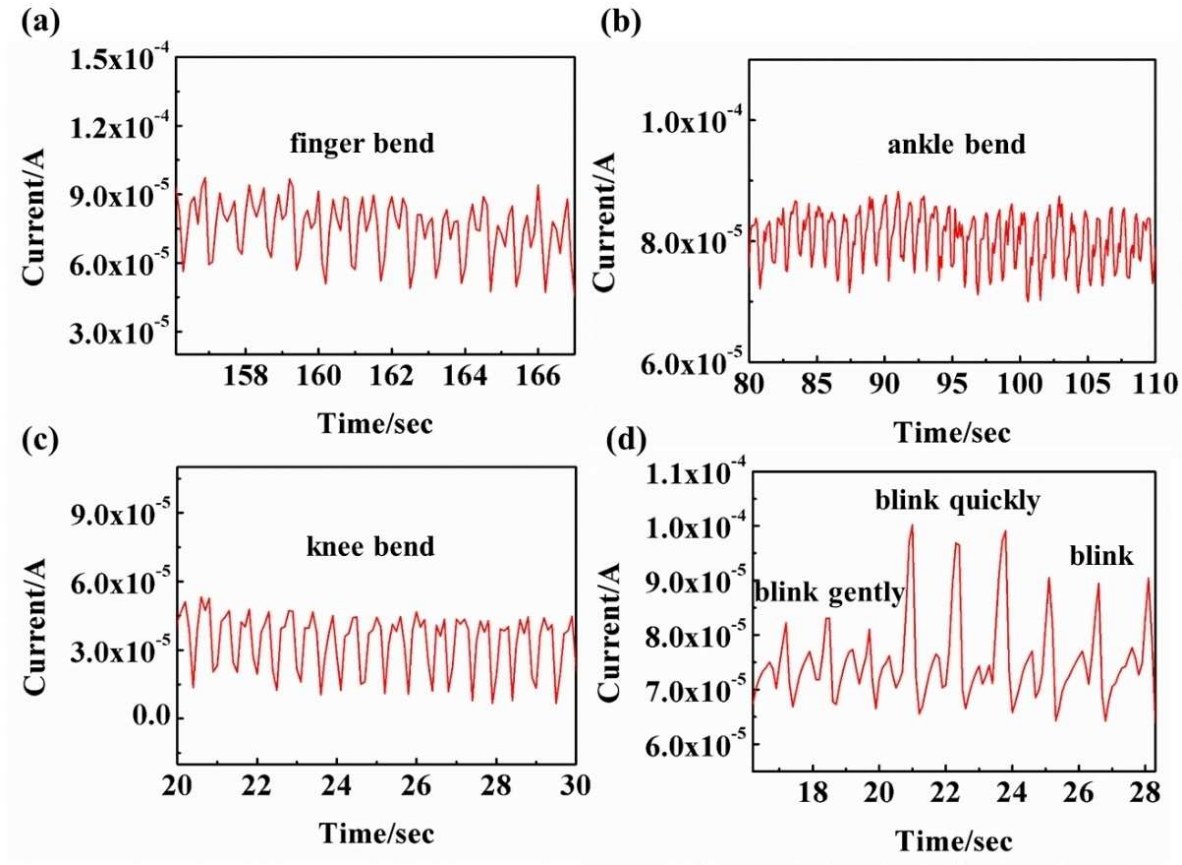

Figure 5. The sensor monitors the dynamic process of current flow during human motion a) Fixing the sensor on the finger measures the change in current as the finger bends. b) Dynamic process of current flow when the sensor is fixed at the ankle to test the in-situ foot. c) Fix the current on the knee when the sensor is fixed on the knee. d) Sensing results of variation of "blink gently", "blink quickly" and "blink" by adhering the sensor on the eye corner.

finally. Some common sports and physiological activities can be monitored in Figure S3c of Supporting Information.

The movement of the human body mostly comes from joints, we attach sensors to body joints and exam some simple activities. The strain sensor can be used to make smart rubber gloves, which can be attached to joints and arrays, practically realizing the sensor's monitoring of human gestures and the degree of finger bending.[44] The application of sensors in man-machine interaction can precisely control the movement of fingers, such as commanding the robot's finger to hit the keyboard and other series of artificial activities.[45] Our AgMFs/PANI/PU sensor was fixed to the knuckle of the finger. The finger was bent at the same amplitude with the same current variation, and the electrochemical workstation showed the current changes throughout the process (Figure 5a). It can be seen that the sensor has good repetitive feedback to the regular bending and works stably. The application of our sensor in man-machine interaction has great potential.

When the person wearing the sensor walks or runs, the change in sensor output signal can be monitored in real time through the sensor. Measurements from a sensor can clarify the state of walking or running, or can count steps accurately. Such an intelligent system can be used for human gait analysis, providing critical clinical treatment and human motion information. Smart systems based on sensors will be a promising technology for assessing the state of the human body during athletic training or competition, as well as physical energy expenditure in daily life.[46] In order to study the response of our sensors to different frequencies, a walking simulation was performed. Figure 5b and 5c show the current change of the sensor at the ankle joint and knee during the simulation of walking, while the two results are unsynchronized. When walking evenly, the current changes steadily and evenly. In Figure 5b, there are 32 peaks of current pulse during 30 seconds, so the step frequency is about 64 steps/min. While the number of peaks is 18 during the 10 seconds in Figure 5c, this means that the step frequency is about 108 steps/min. The frequency of footstep (Figure 5c) is obviously accelerated compared with that in Figure 5b. We can conclude that our sensors can respond well to movements of different frequencies.

When the sensor is attached to one side of the eye, the changes in the electric current are significantly different with blinking speed and frequency. It can be seen that our sensors can give different feedback not only to different frequencies but also to different degrees of deformation.[45] Due to intelligent sensor design, these potential application tests show

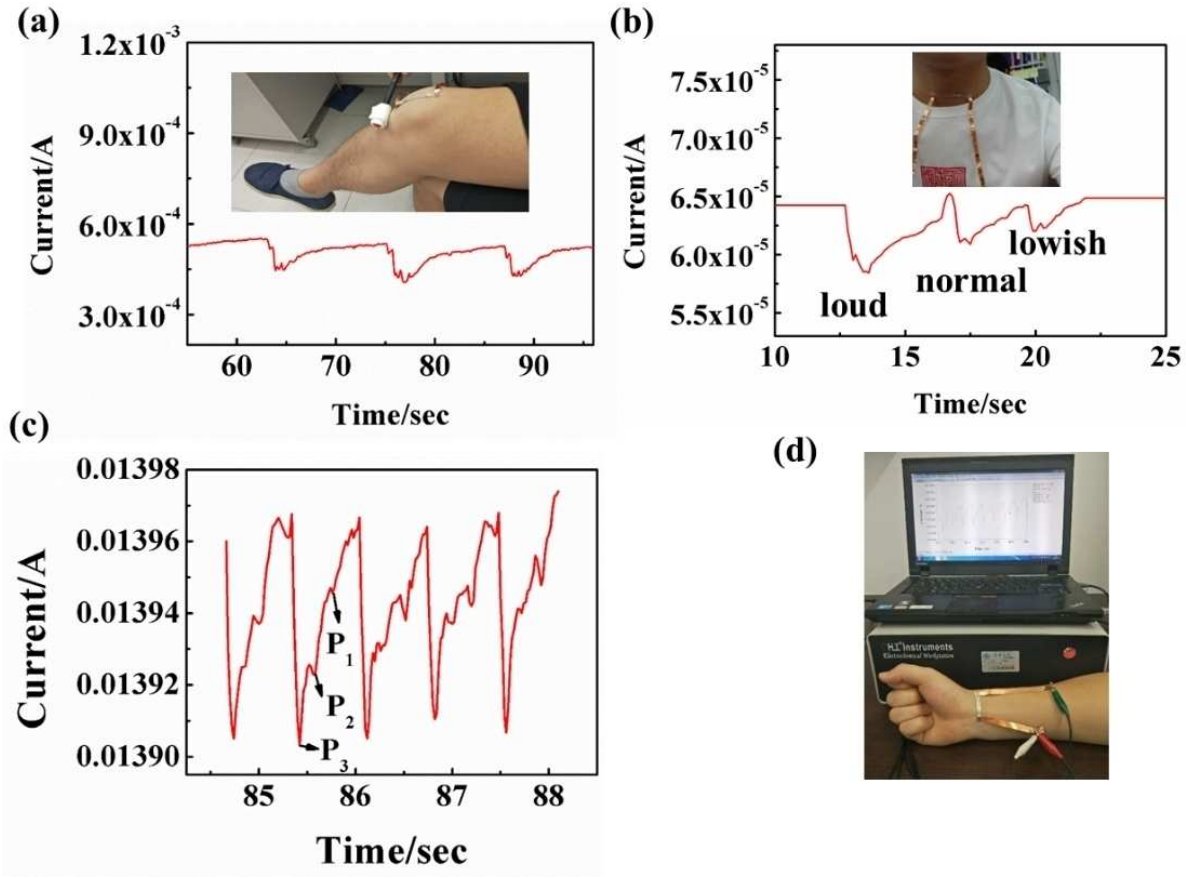

Figure 6. a) Current dynamics during three knee reflexes. b) The current dynamic during the process of reading the word 'sensor' at different volume. c) Monitoring the dynamic process of current during pulse beat at the wrist. d) Photos of the pulse testing process.

great potential in monitoring human activities and clinical medical management.[47]

The sensor not only accurately tests the simple human movement, but also measures some physiological activities of the human body.[48] The obtained data is of great significance in human health monitoring.[49] Sensors can monitor the knee jerk when it is attached to the knee. In a relaxed state, if a small self-made hammer is used to hit the knee below, the lower leg naturally curls up.[50] Figure 6a shows the changes in the sensor current during the three-hop reflex. The same trend is seen in the three current variations, and some details of the oscillations are shown in the figure. Similar variations demonstrate the repeatability and stability of the sensor.[51] Figure 6b shows the sensor's detection of human voice. Vocal cord vibrations cause muscles to contract, which is why we can monitor sound. Read the word "sensor" three times, with the same pronunciation and different volume, result in three similar shapes.[52] Three different volume tests showed that the deformation sensor has the ability of health monitoring in with high repeatability and sensitivity.[53] The strain sensors stand a chance to be used for patients with damaged vocal cords to control the movement of the muscles of the larynx through regular training, which is very helpful for the recovery of the speech ability of the patients with a speech defect.[51]

Figure 6c shows a magnified pulse pressure curve containing a complete current curve with five pulse beats and three clearly distinguishable peaks, which include systolic peak (P_3), reflected systolic peak (P_2), and diastolic peak (P_1).[48] Possible reasons for the relatively weak P_2 peak include changes in heart rate, ventricular ejection characteristics, or the influence of muscular arteries on blood pressure after exercise.[54] The first two peaks, P_3 (t_3) and P_2 (t_2), correspond to two parameters that are most usually used for health monitoring, that is, the radial augmentation index $AIr = P_2/P_3$ and $\Delta TDVP = t_2 - t_3$, t_3 and t_2 are the corresponding times of P_3 and P_2, respectively.[3b] The above results indicate that the strain sensor can monitor minute information of wrist artery pulse, indicating that it has the potential of monitoring very weak signal in the application of real-time monitoring of wearable devices.[54] Figure 6d shows the pulse testing process. For actual wearables, the movement of the wrist affects the accuracy of the measurement. Good mechanical design and strong electrical connections are required to provide stable measurements during motion.[3b] Strain sensors, which rely on human skin deformation or muscle movement, are undoubtedly an interesting and effective method for physiological monitoring, and can be used for the noninvasive diagnosis and treatment of diseases as well as personal healthcare.[51]

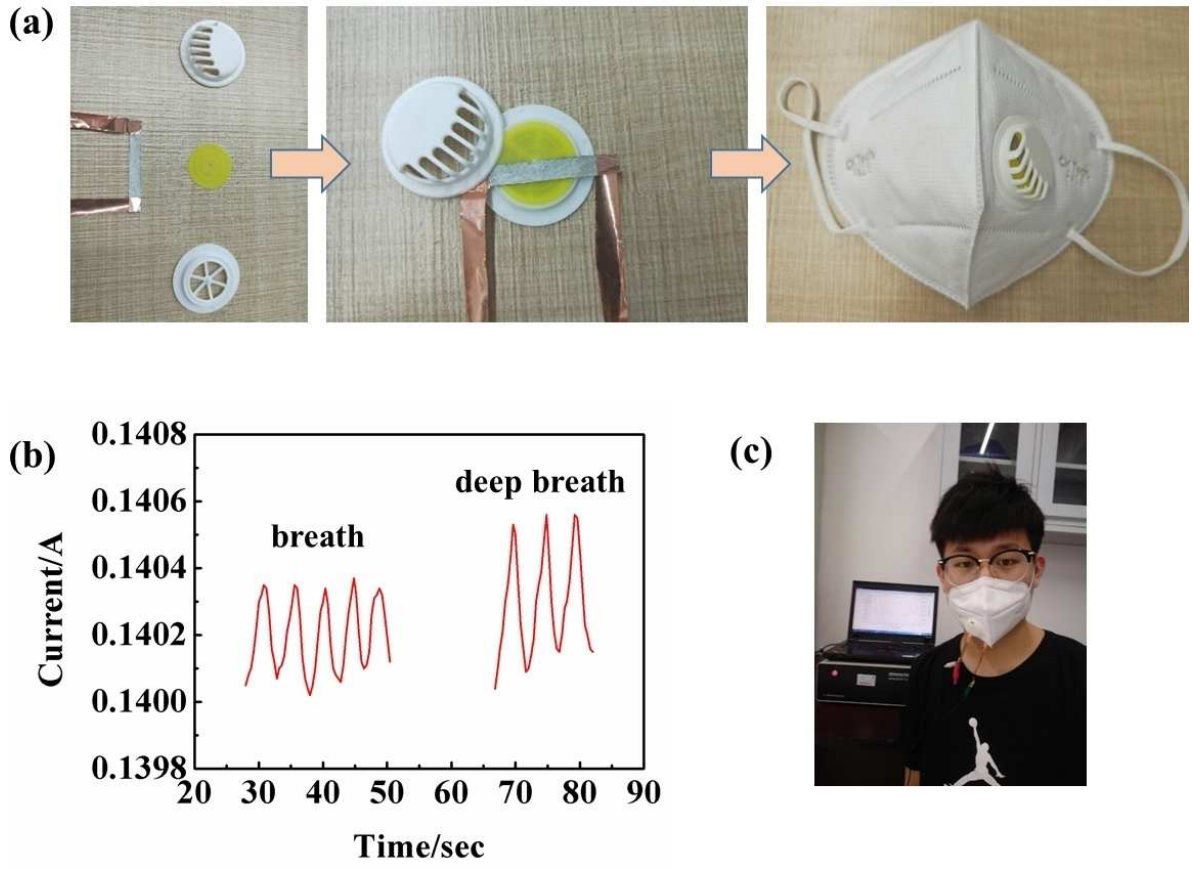

Figure 7. Monitor people's breathing through improved masks a) Improvement process for masks. b) Dynamic changes in current during normal and deep breathing monitored by a mask. c) Photo of the test wearing a mask.

Breathing is an important sign of health. Some researchers have used tubular flow sensors in medical breathing masks to monitor oral breathing. The sensor can monitor different patterns of deep breathing and normal breathing, and changes in resistance during repeated breathing.[55] We explored the potential use of our sensor to monitor human breathing wearable sensor attached on a medical breathing mask. The human respiratory monitoring mask is a simple combination (Figure 7a). Figure 7b shows the current curve of the normal breathing and deep breathing. It is obvious that the range of current change becomes larger when deep breathing, and can be well distinguished from normal breathing. Periodic respiration causes periodic changes in current, whereas different degrees of respiration can also be accurately monitored, indicating that respiration in different respiratory patterns can be recorded and analyzed by sensors. These features open up a lot of possibilities for our sensors, not only with masks in clinical treatment, but also on other medical devices to provide early warning in sudden infant death syndrome.[51]

Simple experiments test the sensor response time, where the time difference between the two inflection points is defined as the response time.[30] The sensor is bent into an arch and fixed on the glass piece, and the same quality millet freely falls at a height of 3, 6, 9 cm respectively. Figure S4 in the Supporting Information shows the dynamic change of the current. When millet hits the sensor, the graph shows a steep slope that drops momentarily. The response is completed in a very short time of 10 ms. The response time of human skin is 50 ms.[30] Our AgMFs/PANI/PU sensor has certain application potential in artificial skin. The sensor can make differential feedback in the face of different impacts. The free fall height of millet is proportional to the difference in current variation, and the difference in current variation increases as the free fall height of millet increases.

3. Conclusion

In this paper, we have obtained highly sensitive **(GF = 173.66)** and fast-response AgMFs/PANI/PU strain sensors in a simple and effective way. Through practical application, it has been confirmed that AgMFs/PANI/PU sensor has a good performance in human monitoring, such as breathing, vocal cords, especially in the monitoring of pulse. It can be seen that AgMFs/PANI/PU sensor has a good sensitivity, and makes an accurate response to some details of human physiological activities. The very short response time enables the AgMFs/PANI/PU strain sensor to monitor high frequency motion. And the AgMFs/PANI/PU strain sensor has great development and application space in

the field of human-computer interaction, flexible electronic skin, and human health monitoring.

Supporting Information

The experimental details, the scheme of the fabrication process of the deformation sensor, SEM images of the AgMFs/PANI/PU, schematic diagram of current measurement, structure diagram of AgMFs/PANI/PU sample, measurement of the millet free fall at different heights and research status of reported flexible strain sensors are presented in the Supporting Information.

Acknowledgements

This work was financially supported by the National Natural Science Foundation of China (No. 11774255), the Key Project of Natural Science Foundation of Tianjin City (No. 17JCZDJC30100). Thanks to Dongxun Yang and Zeyang Chen for their help in drawing Figure S1.

Conflict of Interest

The authors declare no conflict of interest.

Keywords: AgMFs/PANI/PU · flexible · human health monitoring · strain sensor

[1] a) G. Schwartz, B. C. Tee, J. Mei, A. L. Appleton, D. H. Kim, H. Wang, Z. Bao, *Nat. Commun.* **2013**, *4*, 1859; b) X. Wang, Y. Gu, Z. Xiong, Z. Cui, T. Zhang, *Adv. Mater.* **2014**, *26*, 1309; c) G. Shi, Z. Zhao, J.-H. Pai, I. Lee, L. Zhang, C. Stevenson, K. Ishara, R. Zhang, H. Zhu, J. Ma, *Adv. Funct. Mater.* **2016**, *26*, 7614; d) M. Zhang, C. Wang, H. Wang, M. Jian, X. Hao, Y. Zhang, *Adv. Funct. Mater.* **2017**, *27*, 1606066.

[2] a) J. Mu, C. Hou, G. Wang, X. Wang, Q. Zhang, Y. Li, H. Wang, M. Zhu, *Adv. Mater.* **2016**, *28*, 9491; b) H. Stoyanov, M. Kollosche, S. Risse, R. Waché, G. Kofod, *Adv. Mater.* **2013**, *25*, 578.

[3] a) T. Lee, W. Lee, S.-W. Kim, J. J. Kim, B.-S. Kim, *Adv. Funct. Mater.* **2016**, *26*, 6206; b) Y. Si, X. Wang, C. Yan, L. Yang, J. Yu, B. Ding, *Adv. Mater.* **2016**, *28*, 9655.

[4] A. P. Gerratt, H. O. Michaud, S. P. Lacour, *Adv. Funct. Mater.* **2015**, *25*, 2287.

[5] T. Yan, Z. Wang, Z.-J. Pan, *J. Mater. Sci.* **2018**, *53*, 11917.

[6] Z. Yuan, Y. Hu, Z. Tao, P. Zhu, S. Rong, C. Wong, Z. Yuan, Y. Hu, Z. Tao, P. Zhu, *ICEPT* **2017**.

[7] I. Kim, K. Woo, Z. Zhong, P. Ko, Y. Jang, M. Jung, J. Jo, S. Kwon, S. H. Lee, S. Lee, H. Youn, J. Moon, *Nanoscale* **2018**, *10*, 7890.

[8] M. Li, H. Li, W. Zhong, Q. Zhao, D. Wang, *ACS Appl. mater. Interfaces* **2014**, *6*, 1313.

[9] J. Liu, D. Ma, Z. Li, *Eur. Polym. J.* **2002**, *38*, 661.

[10] Z. Ma, A. Wei, J. Ma, L. Shao, H. Jiang, D. Dong, Z. Ji, Q. Wang, S. Kang, *Nanoscale* **2018**, *10*, 7116.

[11] X. Guo, H. Ying, Y. Zhao, L. Mao, G. Le, W. Pan, Y. Zhang, L. Ping, *Smart Mater. Struct.* **2017**, *26*, 095017.

[12] L. V. Grigoryev, S. V. Kulakov, V. G. Nefedov, O. V. Shakin, M. L. Grigoryeva, S. D. Moskalenko, *J. Phys. Confer. S.* **2017**, *857*, 012011.

[13] J. B. Chaudhari, R. S. Patil, I. J. Patil, P. P. Jagtap, R. Sharma, *Am. Inst. Phys. Conf. Ser.* **2012**.*1447*, 697.

[14] I. Kim, K. Woo, Z. Zhong, P. Ko, Y. Jang, M. Jung, J. Jo, S. Kwon, S. H. Lee, S. Lee, *Nanoscale* **2018**, *10*, 7890.

[15] T. Araki, M. Nogi, K. Suganuma, M. Kogure, O. Kirihara, *IEEE Electron Device Lett.* **2011**, *32*, 1424.

[16] a) J. E. Q. Quinsaat, M. Alexandru, F. A. Nüesch, H. Hofmann, A. Borgschulte, D. M. Opris, *J. Mater. Chem. A* **2015**, *3*, 14675; b) K. Takei, Z. Yu, M. Zheng, H. Ota, T. Takahashi, A. Javey, *Proc. Natl. Acad. Sci. U. S. A.* **2014**, *111*, 1703.

[17] a) G. Shu, D. T. H. Lai, B. Su, K. J. Si, M. Zheng, L. W. Yap, P. Guo, W. Cheng, *Adv. Electron. Mater.* **2015**, *1*, 1400063; b) S. Yao, Y. Zhu, *Nanoscale* **2014**, *6*, 2345.

[18] a) Alamusi, N. Hu, H. Fukunaga, S. Atobe, Y. Liu, J. Li, *Sensors* **2011**, *11*, 10691; b) M. Ji, D. Hua, D. Yan, X. Li, L. Duan, F. Qiang, *Compos. Sci. Technol.* **2014**, *92*, 16.

[19] Y. Lin, X. Dong, S. Liu, S. Chen, Y. Wei, L. Liu, *ACS Appl. mater. Interfaces* **1944**, *8*, 24143.

[20] L. Zhuo, Y. Yao, Z. Lin, K. S. Moon, L. Wei, C. Wong, *J. Mater. Chem.* **2010**, *20*, 4781.

[21] N. Matsuhisa, M. Kaltenbrunner, T. Yokota, H. Jinno, K. Kuribara, T. Sekitani, T. Someya, *Nat Commun* **2015**, *6*, 7461.

[22] T. Araki, M. Nogi, K. Suganuma, M. Kogure, O. Kirihara, *IEEE Electron Device Lett.* **2011**, *32*, 1424.

[23] I. Kim, K. Woo, Z. Zhong, P. Ko, Y. Jang, M. Jung, J. Jo, S. Kwon, S. H. Lee, S. Lee, H. Youn, J. Moon, *Nanoscale* **2018**, *10*, 7890.

[24] Y. X. Song, W. M. Xu, M. Z. Rong, M. Q. Zhang, *J. Mater. Chem. A* **2019**, *7*, 2315.

[25] B. Tian, W. Yao, P. Zeng, X. Li, W. Wu, *J. Mater. Chem. C* **2019**, *7*, 809.

[26] C. Yang, X. Cui, Z. Zhang, S. W. Chiang, W. Lin, H. Duan, J. Li, F. Kang, C. P. Wong, *Nat. Commun.* **2015**, *6*, 8150.

[27] J. Njuguna, K. Pielichowski, *J. Mater. Sci.* **2004**, *39*, 4081.

[28] a) Y. C. Long, L. Y. Wang, C. S. Kuo, J. G. Lin, C. Y. Huang, *Synth. Met.* **1997**, *84*, 721; b) Y. Wang, H. D. Tran, L. Liao, X. Duan, R. B. Kaner, *J. Am. Chem. Soc.* **2010**, *132*, 10365.

[29] N. Matsuhisa, D. Inoue, P. Zalar, H. Jin, Y. Matsuba, A. Itoh, T. Yokota, D. Hashizume, T. Someya, *Nat. Mater.* **2017**, *16*, 834.

[30] C. Li, L. Pan, C. Deng, P. Wang, Y. Huang, H. Nasir, *Nanoscale* **2017**, *9,* 9872.

[31] a) G. E. Pike, C. H. Seager, *Phys. Rev. B* **1974**, *10*, 1421; b) A. S. Ioselevich, A. A. Kornyshev, *Phys. Rev. E* **2002**, *65*, 021301.

[32] H. Ma, J. Zeng, S. Harrington, M. Lei, M. Ma, X. Guo, Y. Ma, *Nanomaterials* **2016**, *6*, 119.

[33] C. Li, L. Pan, C. Deng, P. Wang, Y. Huang, H. Nasir, *Nanoscale* **2017**, 9, 9872.

[34] T. Yan, Z. Wang, Y. Q. Wang, Z. J. Pan, *Mater. Des.* **2018**, *143*, 214.

[35] Y. Lin, S. Liu, S. Chen, Y. Wei, X. Dong, L. Liu, *J. Mater. Chem. C* **2016**, *4*, 6345.

[36] J. Lee, S. Shin, S. Lee, J. Song, S. Kang, H. Han, S. G. Kim, S. Kim, J. Seo, D. E. Kim, *ACS Nano* **2018**, *12*, 4259.

[37] D. Hongbo, E. T. Thostenson, S. Thomas, *Sensors* **2015**, *15*, 17728.

[38] J. Shi, X. Li, H. Cheng, Z. Liu, L. Zhao, T. Yang, Z. Dai, Z. Cheng, E. Shi, L. Yang, *Adv. Funct. Mater.* **2016**, *26*, 2078.

[39] T. Yang, X. Jiang, Y. Zhong, X. Zhao, S. Lin, J. Li, X. Li, J. Xu, Z. Li, H. Zhu, *ACS Sens.* **2017**, *2*, 967.

[40] M. B. Coskun, A. Akbari, D. Lai, A. Neild, M. Majumder, T. Alan, *ACS Appl. mater. Interfaces* **2016**, *8*, 22501.

[41] C. J. Lee, K. H. Park, C. J. Han, S. O. Min, B. You, Y. S. Kim, J. W. Kim, *Sci. Rep.* **2017**, *7*, 7959.

[42] S. Sang, L. Liu, A. Jian, Q. Duan, J. Ji, Q. Zhang, W. Zhang, *Nanotechnology* **2018**, *29*, 255202.

[43] X. Wang, G. Yang, Z. Xiong, C. Zheng, T. Zhang, *Adv. Mater.* **2014**, *26*, 1309.

[44] H. J. Kim, A. Thukral, C. Yu, *ACS Appl. mater. Interfaces* **2018**, *10*, 5000.

[45] J. Kim, M. Lee, H. J. Shim, R. Ghaffari, H. R. Cho, D. Son, Y. H. Jung, M. Soh, C. Choi, S. Jung, *Nat. Commun.* **2013**, *5*, 5747.

[46] S. Chen, B. Zhuo, X. Guo, *ACS Appl. mater. Interfaces* **2016**, *8*, 20364.

[47] W. Zhong, C. Liu, C. Xiang, Y. Jin, M. Li, K. Liu, Q. Liu, Y. Wang, G. Sun, D. Wang, *ACS Appl. mater. Interfaces* **2017**, *11*, 8790.

[48] R. Li, Y. Si, Z. Zhu, Y. Guo, Y. Zhang, N. Pan, G. Sun, T. Pan, *Adv. Mater.* **2017**, *29*, 1700253.

[49] K. Dong, S. Hong, Y. Deng, H. Ma, J. Li, X. Wang, J. Yeo, L. Wang, S. Lou, K. B. Tom, *Adv. Mater.* **2018**, *30*, 1703878.

[50] E. G. Hamer, L. J. Dijkstra, S. J. Hooijsma, I. Zijdewind, M. Haddersalgra, *Pediatr. Res.* **2016**, *80*, 363.

[51] J. Deng, X. Kuang, R. Liu, W. Ding, A. C. Wang, Y. C. Lai, K. Dong, Z. Wen, Y. Wang, L. Wang, *Adv. Mater.* **2018**, *30*, 1705918.

[52] Z. Yang, D. Y. Wang, Y. Pang, Y. X. Li, Q. Wang, T. Y. Zhang, J. B. Wang, X. Liu, Y. Y. Yang, J. M. Jian, *ACS Appl. mater. Interfaces* **2017**, *11*, 8790.
[53] L. Zheng, C. Shuai, L. Wang, R. Shi, L. Li, J. Kai, C. Di, G. Shen, *Nano Energy* **2017**, *38*, 28.
[54] Y. Zang, F. Zhang, D. Huang, X. Gao, C. Di, D. Zhu, *Nat. Commun.* **2015**, *6*, 6269.
[55] J. Park, Y. Lee, J. Hong, Y. Lee, M. Ha, Y. Jung, H. Lim, S. Y. Kim, H. Ko, *ACS Nano* **2014**, *8*, 12020.

Submitted: February 12, 2019
Accepted: March 31, 2019